Resonance acceleration of electrons in combined strong magnetic fields and intense laser fields

Hong Liu,[1,4,*] X. T. He,[2,3] and S. G. Chen[2]
[1]*Graduate School, China Academy of Engineering Physics, Beijing P. O. Box 2101, Beijing 100088, People's Republic of China*
[2]*Institute of Applied Physics and Computational Mathematics, Beijing P. O. Box 8009, Beijing 100088, People's Republic of China*
[3]*Department of Physics, Zhejiang University, Hangzhou 310027, People's Republic of China*
[4]*Basic Department, Beijing Material College, Beijing 101149, People's Republic of China*
(Received 25 June 2003; revised manuscript received 17 October 2003; published 11 June 2004)

The acceleration mechanism of electrons in combined strong axial magnetic fields and circularly polarized laser pulse fields is investigated by solving the dynamical equations for relativistic electrons both numerically and analytically. We find that the electron acceleration depends not only on the laser intensity, but also on the ratio between electron Larmor frequency and laser frequency. As the ratio approaches unity, a clear resonance peak is observed, corresponding to the laser-magnetic resonance acceleration. Away from the resonance regime, the strong magnetic fields still affect the electron acceleration dramatically. We derive an approximate analytical solution of the relativistic electron energy in adiabatic limit, which provides a full understanding of this phenomenon. Application of our theory to fast ignition of inertial confinement fusion is discussed.

DOI: 10.1103/PhysRevE.69.066409 PACS number(s): 52.38.Kd, 41.75.Lx

I. INTRODUCTION

Recently, strong magnetic fields have achieved much attention in laser-matter interaction [1] and other physical fields [2]. An interesting question of how strong quasistatic magnetic fields influence electron acceleration has been discussed extensively, e.g., *B*-loop acceleration of Pukhov and Meyer-ter-Vehn [3], direct electron acceleration of Tanimoto *et al.* [4]. Here, the strong magnetic fields are generated by high electron current during short-pulse high-intense laser-plasma interactions [5], namely, spontaneous magnetic fields [6,7]. It is observed that a linearly polarized (LP) laser pulse can only generate quasistatic toroidal magnetic fields [4,8], whereas a circularly polarized (CP) laser pulse can generate toroidal as well as axial magnetic fields [7,9]. A recent experiment [10] has measured dc 3.4×10^8 G magnetic field on the surface of solid target in the LP laser-plasma interaction. Much higher magnetic field of strength up to 10^{12} G has been found on the surface of neutron stars [2].

On the other hand, in the fast ignition scheme [11] of inertial confinement fusion (ICF), the production of collimating electrons with moderate energy (<2 MeV) is a key point. Therefore, how the spontaneous magnetic fields affect election acceleration and electron collimation is a problem of great interest. Although experiments [12,13] and three-dimensional (3D) particle-in-cell (PIC) simulations [14] clearly demonstrate that the fact of strong currents of energetic 10–100 MeV electrons manifest themselves in a giant quasistatic magnetic field with up to 100 MG amplitude, the electrons with such high energy do not easily stop in highly compressed deuterium tritium (DT) fuel core for fast ignition. To our knowledge, on these topics linearly polarized short-pulse and high-intense lasers have been intensely considered in theoretical and experimental studies.

In studying the acceleration of electrons, the single test electron model is a simple but effective one. It has been used to analyze the direct laser acceleration of relativistic electrons in plasma channels. For example, Schmitz and Kull [15] have analyzed the LP laser system with self-generated static electric field and discussed the electron resonant acceleration mechanism. Even though the simple model is not fully self-consistent, it can help us achieve essential insight into the physical process of electron acceleration involved in the laser-plasma interactions. In this paper, we extend this study to consider combined CP laser fields and strong magnetic fields, exploiting the single test electron model to investigate the electron acceleration. We also discuss laser-magnetic resonance acceleration (LMRA) mechanism of electrons in strong laser and axial magnetic fields. In our simulation, the laser field is a Gaussian profile. The axial magnetic field is considered as a constant field and a quassistatic field with Gaussian profile, respectively. A fully relativistic single particle code is developed to investigate the dynamical properties of the energetic electrons. We find a big difference between the CP laser case and the LP laser case. In the CP laser system there is only one resonance peak, but in the LP laser system there are two resonance peaks. More importantly, at the magnetic field corresponding to the disappeared resonance peak, we find that energetic electrons can be successively collimated and accelerated to a moderate energy <2 MeV. This kind of electrons have potential application in the fast-ignitor scheme of ICF.

Our paper is organized as follows. In Sec. II, we derive the dynamical equations describing relativistic electrons in combined strong axial magnetic fields and the CP laser fields. These equations will be solved both numerically and analytically. We describe LMRA in a Gaussian CP beam with static axial magnetic field. An approximately analytical solution of relativistic electron energy is obtained, which gives a good explanation for our numerical simulations. This equation also suits a Gaussian profile quasistatic axial magnetic field which is considered as a spontaneous axial magnetic field. Our discussion and conclusion are given in Sec. III. The potential applications in fast ignition scheme of ICF are also discussed.

*Email address: Liuhong_cc@yahoo.com.cn

 ©2004 The American Physical Society

II. GAUSSIAN CP LASER PULSE MODEL

In this section, we use 3D test electron model to simulate electron acceleration in plasma channel, i.e., a cylindrically symmetric plasma with a uniform charge density n and a uniform current density $\mathbf{j}$ along the z axis. Here, we assume that the electrons have been partially expelled from the channel by the ponderomotive force. The focused laser pulse with frequency ω propagates in positive $\hat{\mathbf{z}}$ direction along the channel with a phase velocity v_{ph}. The corresponding electromagnetic fields $\mathbf{E}=-\nabla\Phi-\partial_t\mathbf{A}/c$ and $\mathbf{B}=\nabla\times\mathbf{A}$ are derived from potentials Φ and $\mathbf{A}$ by

$$\frac{e\Phi}{mc^2} = -\frac{1}{2}k_E(kr)^2, \tag{1}$$

$$\frac{e\mathbf{A}}{mc^2} = \mathbf{a} - \frac{1}{2}k_B(\hat{\mathbf{x}}y - \hat{\mathbf{y}}x), \tag{2}$$

where m denotes the electron mass, $-e$ the electron charge, c the light velocity, and $k=\omega/c$, $r=\sqrt{x^2+y^2}$. The model contains three dimensionless parameters,

$$k_E = \frac{n}{2en_c}, \quad k_B = \frac{|\mathbf{j}|}{2en_cc}, \tag{3}$$

$$\begin{aligned}\mathbf{a} &= a_0 e^{-(x^2+y^2)/R_0^2} e^{-(kz-\omega t)^2/k^2L^2}[\cos(\omega t - kz)\hat{\mathbf{x}} \\ &\quad + \delta\sin(\omega t - kz)\hat{\mathbf{y}}] \\ &= a_x + \delta a_y,\end{aligned} \tag{4}$$

where the critical density $n_c=m\omega^2/(4\pi e^2)$, the plasma frequency equals the light frequency, and L and R_0 are the pulse width and minimum spot size, respectively. The two components of the laser amplitude $\mathbf{a}$ take the form $a_x=a_0e^{-(x^2+y^2)/R_0^2}e^{-(kz-\omega t)^2/k^2L^2}[\cos(\omega t-kz)]$ and $a_y=a_0e^{-(x^2+y^2)/R_0^2}e^{-(kz-\omega t)^2/k^2L^2}[\sin(\omega t-kz)]$, respectively.

For the irradiance of the femtosecond laser pulses, the plasma ions have no time to respond to the laser and therefore can be assumed to be immobile. δ equals 0, 1, and −1, corresponding to linear, right-hand, and left-hand circular polarization, respectively. For simplicity, in the following discussions we assume that the phase velocity of the laser pulse equals the light velocity, i.e., $v_{ph}=c$. The main results obtained can be readily extended to the case of $v_{ph}\neq c$.

To describe an axial spontaneous quasistatic magnetic field that exists in the relativistic CP laser-plasma interaction systems [7,9], we use following approximate expression:

$$\mathbf{b}_z = -\delta b_{z0}|a|^2\hat{\mathbf{z}}, \tag{5}$$

where b_{z0} is a parameter, its value can be fitted by numerical simulations or practical experiments.

We first consider a static axial magnetic field and then extend our conclusion to a Gaussian profile quasistatic axial magnetic field. The above explicit expression clearly indicates that the self-generated magnetic field $\mathbf{b}_z$ is oriented along the negative laser propagation direction for the right-hand circular polarization ($\delta=1$). For left-hand circular polarization ($\delta=-1$), the self-generated magnetic field $\mathbf{b}_z$ is oriented along the laser propagation direction. Obviously, for the LP laser beam ($\delta=0$) there is no spontaneous magnetic field along the axial direction. Horovitz *et al.* [16] and Najmudin *et al.* [17] have measured the axial magnetic field $\mathbf{b}_z$ for the intense CP lasers. They found that, in underdense helium plasma the maximum strength of the magnetic field is of the order 10 kG for the laser intensity 10^{13}–10^{14} W/cm^2, and of the order 7 MG for the laser intensity 10^{19} W/cm^2, respectively. For near-overdense plasma, the peak value of the self-generated magnetic field is around hundreds of MG from the theoretical analysis [7]. The spatial distribution of the axial magnetic field $\mathbf{b}_z$ takes the same Gaussian shape as a^2, as plotted in Fig. 1. For convenience, we first consider the simplest case of the constant magnetic field, i.e., $b_z=k_B=const$. The case with Gaussian profile of $\mathbf{b}_z$ will be discussed later for comparison.

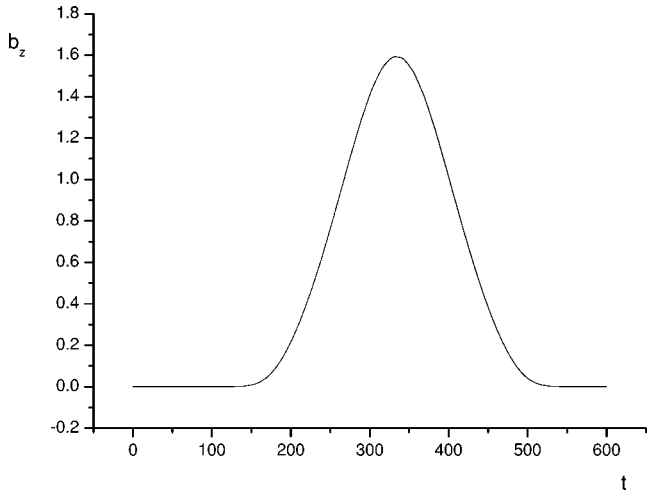

FIG. 1. The profile of a rough spontaneous quasistatic magnetic field (units=100 MG) as a function of time (in the units of ω^{-1}) generated by a left-hand Gaussian profile CP laser (propagation is in positive $\hat{\mathbf{z}}$ direction).

To discuss the acceleration of electrons in the channel, we consider the dynamical equations,

$$\frac{d\mathbf{p}}{dt} = -e\left(\mathbf{E} + \frac{1}{c}\mathbf{v}\times\mathbf{B}\right), \tag{6}$$

with the relativistic momentum,

$$\mathbf{p} = \gamma m\mathbf{v}, \quad \gamma = \frac{1}{\sqrt{1-v^2/c^2}}. \tag{7}$$

We assume that the trajectory of a test electron starts at $\mathbf{v}_0=0$. Equation (1) and (2) yield

$$\frac{dp_x}{dt} = (v_z-1)\frac{\partial a_x}{\partial z} + v_y\left(\frac{\partial a_x}{\partial y} - \delta\frac{\partial a_y}{\partial x}\right) - v_yb_z - k_Ex, \tag{8}$$

$$\frac{dp_y}{dt} = (v_z-1)\delta\frac{\partial a_y}{\partial z} + v_x\left(\delta\frac{\partial a_y}{\partial x} - \frac{\partial a_x}{\partial y}\right) + v_xb_z - k_Ey, \tag{9}$$

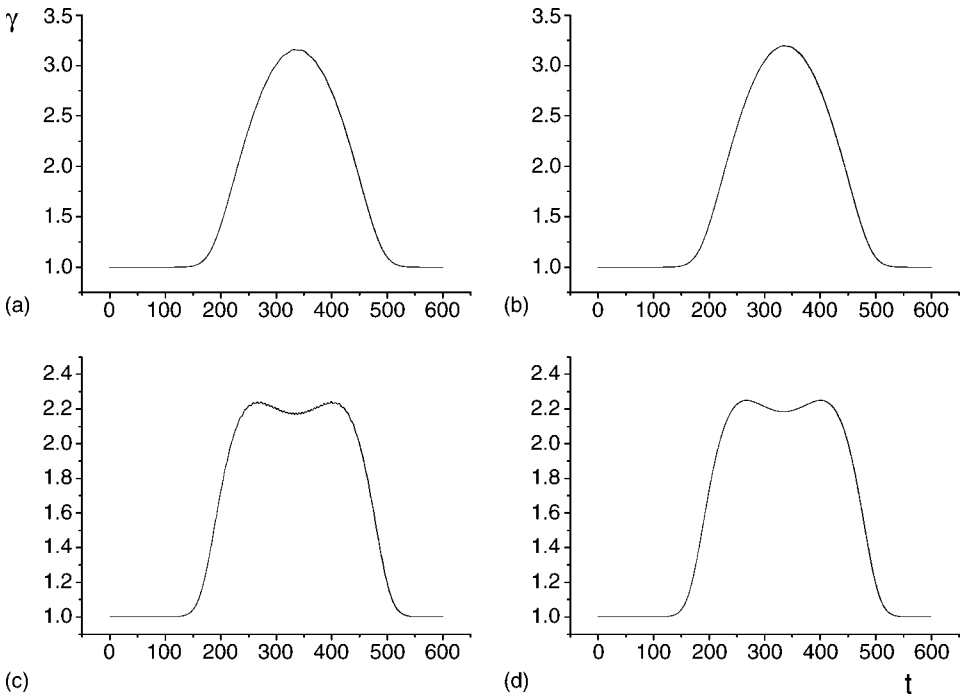

FIG. 2. The electron energy γ in units of mc^2 as a function of time in the units of ω^{-1} of the CP laser. (a) and (c) The numerical solutions by the Eqs. (8)–(10). (b) and (d) The analytical solutions by Eq. (19). The parameters $\delta=-1$, $a_0=4$, $k_E=0$, $\mathbf{r}_0=0.1$ (in the units of k^{-1}), $\mathbf{v}_0=0$, for the static case $b_z=k_B=0.9$ (corresponding to $B_z=90$ MG) shown in (a) and (b), for the Gaussian profile case B_z ($|b_{z0\ \max}|=1.6$ corresponding to $B_{z\ \max}=160$ MG) shown in (c) and (d).

$$\frac{dp_z}{dt} = -v_x\frac{\partial a_x}{\partial z} - v_y\delta\frac{\partial a_y}{\partial z}, \tag{10}$$

$$\frac{d\gamma}{dt} = -v_x\frac{\partial a_x}{\partial z} - v_y\delta\frac{\partial a_y}{\partial z} - k_E x v_x - k_E y v_y, \tag{11}$$

where we have used the dimensionless variables

$$\mathbf{a} = \frac{e\mathbf{A}}{m_e c^2}, \quad \Phi = \frac{e\Phi}{m_e c^2}, \quad \mathbf{b} = \frac{e\mathbf{B}}{m_e c\omega}, \quad \mathbf{v} = \frac{\mathbf{u}}{c},$$

$$\mathbf{p} = \frac{\mathbf{p}}{m_e c} = \gamma\mathbf{v}, \quad t = \omega t, \quad r = kr. \tag{12}$$

Using Eqs. (8)–(10), we choose different initial positions to investigate the electron dynamics for a Gaussian profile laser pulse. We first neglect the static electric field for simplicity. Because initial velocity can be transformed to initial position in our single test electron case, we keep the initial velocity at rest and change the initial positions of the test electrons. We assume that the trajectory of a test electron starts from $\mathbf{v}_0=0$ and $z_0=4$ L at $t=0$, while the center of laser pulse locates at $z=0$, then the classical trajectory is fully determined by Eqs. (8)–(10). Now we choose following parameters that are available in present experiments, i.e., $L=10\lambda$, $R_0=5\lambda$ ($\lambda=1.06$ μm), $\delta=-1$, $a_0=4$ (corresponding to $I=2\times10^{19}$ W/cm^2), $k_E=0$, $\mathbf{r}_0=0.1$. We then trace the temporal evolution of electron energy, i.e., $\gamma\sim t$, and plot the results in Fig. 2.

Obtaining an exactly analytical solution of Eqs. (8)–(11) is impossible because of their nonlinearity. However, we notice that the second term on the left side of Eqs. (8) and (9) possesses symmetric form, which is found to be a negligibly small quantity after careful analysis. Then, approximately analytical solutions of Eqs. (8)–(11) in adiabatic limit can be obtained after setting $k_E=0$.

We first consider the right-hand CP laser. From the phase of the laser pulse, we have the equation,

$$\frac{d\eta}{dt} = \omega(1 - v_z), \tag{13}$$

where $\eta=\omega t-kz$. Then, from Eqs. (10) and (11), we can easily arrive at the second useful relation under the initial condition $\mathbf{v}_0=0$ at $t=0$,

$$\gamma v_z = \gamma - 1. \tag{14}$$

Finally, the energy-momentum equation yields

$$\gamma^2 = 1 + (\gamma v_x)^2 + (\gamma v_y)^2 + (\gamma v_z)^2. \tag{15}$$

The solution of the electron momentum has symmetry. In adiabatic limit and under the initial condition of zero velocity electron, we find the solutions of Eqs. (8) and (9) taking the form,

$$\omega p_x = -b_z\cos(\omega t - kz), \tag{16}$$

$$\omega p_y = b_z\sin(\omega t - kz). \tag{17}$$

Substituting Eqs. (16) and (17) into Eq. (8), and using Eqs. (13)–(15), we obtain an equation having a resonance point (singularity) at a positive $b_z(=\omega)$,

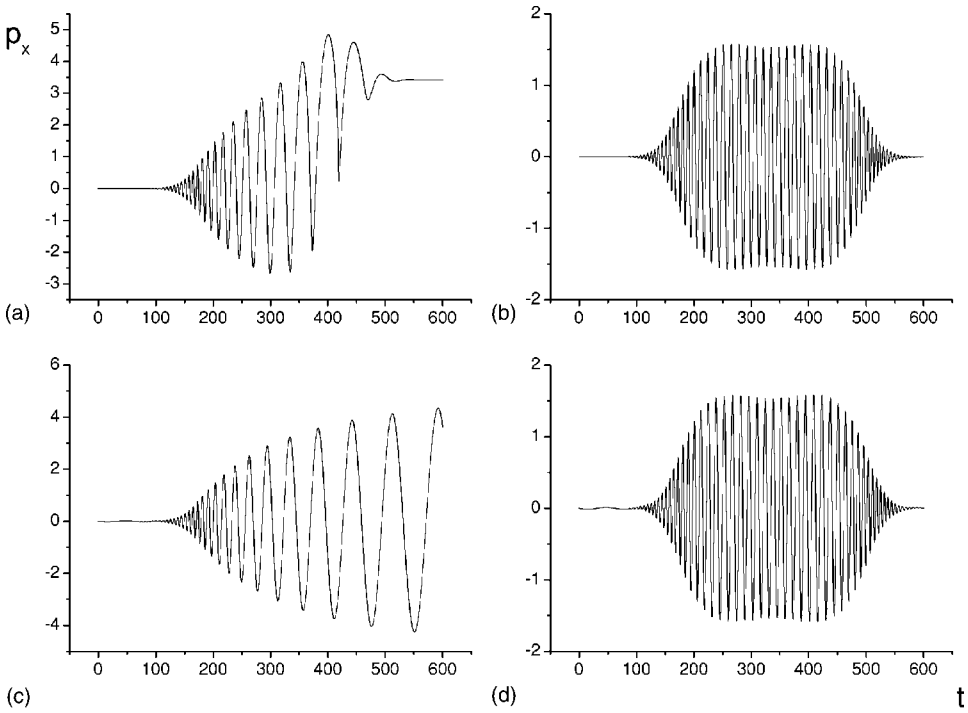

FIG. 3. The transverse momentum p_x in units of mc as a function of time in the units of ω^{-1} of the CP laser. The initial dimensionless parameters $\mathbf{v}_0=0$, $x_0=0.1$, $y_0=0$, and the dimensionless field parameters (a) $a_0=4$, $b_z=k_E=0$, (b) $a_0=4$, $b_z=1.6$, $k_E=0$, (c) $a_0=4$, $b_z=0$, $k_E=0.01$, (d) $a_0=4$, $b_z=1.6$, $k_E=0.01$.

$$\gamma = 1 + \frac{1}{2}\frac{a^2}{\left(1-\frac{b_z}{\omega}\right)^2}. \tag{18}$$

The same steps can be repeated for the left-hand CP laser, the solution with a resonance point in the negative b_z is then obtained,

$$\gamma = 1 + \frac{1}{2}\frac{a^2}{\left(1+\frac{b_z}{\omega}\right)^2}. \tag{19}$$

Equations (18) and (19) are approximately analytical energy solutions of Eqs. (8)–(11). For the left-hand CP laser, the analytic results of $\gamma \sim t$ from Eq. (19) are shown in Fig. 2(b) for $b_z=k_B=0.9$, and in Fig. 2(d) for $|b_{z0\ \max}|=1.6$ (Gaussian profile). From the above analytic solutions and our numerical calculations, we find that the strong self-generated magnetic fields reduce the maximum energy gain and produce a local minimum in $\gamma \sim t$ curves, which can be clearly seen by comparing Figs. 2(a) and 2(b) with Figs. 2(c) and 2(d).

In order to get an analytical expression of electron energy γ at the exact resonance point ($b_z=\omega$), we plug following the approximate solutions into the dynamical equations:

$$\omega p_x = c(t)\sin(\omega t - kz), \tag{20}$$

$$\omega p_y = c(t)\cos(\omega t - kz), \tag{21}$$

where $c(t)$ is a coefficient to be fitted. Careful analysis gives the solution at $t \to \infty$ in the following approximate expression

$$\gamma \approx \left(\frac{3}{\sqrt{2}}a\omega t\right)^{2/3}. \tag{22}$$

It indicates that the resonance between the laser fields and magnetic fields will drive the energy of electrons to infinity with a $2/3$ power law in time. But in actual experimental conditions, Eq. (22) is hard to occur.

When the self-generated static electric field is considered, the resonant acceleration of electron can occur as well. This has been analyzed by Schmitz and Kull [15]. In order to compare it with our LMRA mechanism, we plot the numerical solutions in Figs. 3–5 for (a) CP laser field, (b) CP laser field and quasistatic $\mathbf{b}_z$, (c) CP laser field and static electric field, (d) CP laser field, quasistatic $\mathbf{b}_z$, and static electric field. Figure 3 shows the temporal evolution of the transverse momentum $p_x(t)$. The initial conditions $\mathbf{v}_0=0$, $x_0=0.1$, $y_0=0$, and the field parameters are (a) $a_0=4$, $b_z=k_E=0$, (b) $a_0=4$, $b_z=1.6$, $k_E=0$, (c) $a_0=4$, $b_z=0$, $k_E=0.01$, (d) $a_0=4$, $b_z=1.6$, $k_E=0.01$. Figure 4 shows the evolution of the energy $\gamma(t)$. Figure 5 shows the 3D trajectories of the electrons.

It is well known, in off-resonance regime, e.g., around $b_z=0$, a Gaussian-wave pulse can accelerate electrons and the accelerated electron has a large scattering angle [18]. This is the so-called ponderomotive scattering, as shown in Figs. 3–5(a). We like to emphasize that at relativistic intensities laser ($I>10^{18}$ W/cm^2) the electron drift velocity is very slow but not slow enough. In fact, for $a_0=2$ the drift velocity is the same order as the quiver velocity. When $a_0=4$, $\mathbf{p}_\perp=\mathbf{a}$, $p_z=a^2/2$ from $\gamma=\sqrt{1+p_\perp^2+p_z^2}$, then $\gamma_{\max}=9$. The nonlinear ponderomotive scattering angle (in vacuum) $\theta=\arctan\sqrt{2/(\gamma-1)}\approx 28°$. Such large scattering angles will be unfavorable to the fast ignition of the high compressed fuel.

When a strong self-generated axial magnetic field exists, from analytic solutions Eqs. (18) and (19), the magnetic field

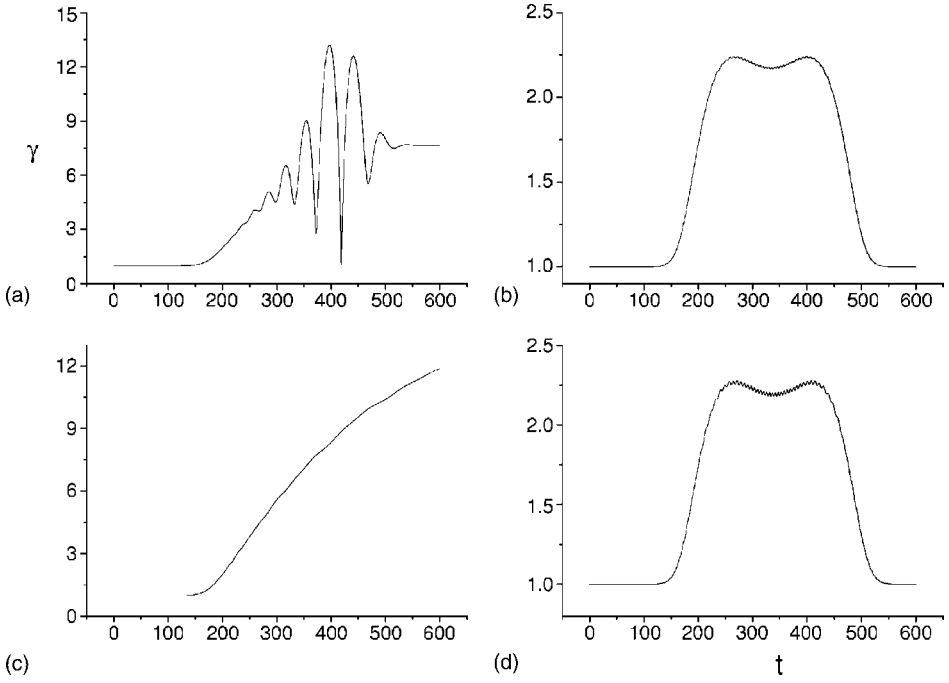

FIG. 4. The electron energy γ in units of mc^2 as a function of time in the units of ω^{-1} with the same parameters of Figs. 2(a)–2(d), respectively.

will reduce the longitudinal and transverse momentum of the electrons, as shown in Figs. 3–5(b). The electrons that initially locate on the center axis of the laser beam will move around z axis. The maximum electron energy (<2 MeV) can be calculated from Eqs. (18) and (19) and can also be found from $\gamma \sim t$ curve in Fig. 4(b). From the above discussions we find that strong axial magnetic fields will influence the electron motion and change the distribution in the three velocity components of the electrons. The existence of dc axial magnetic field changes the scattering angle of accelerated electron dramatically. It provides a guiding center for the accelerated electrons, and finally can collimate the electrons.

Figures 3–5(c) show the resonant acceleration in presence of a static electric field ($k_E=0.01$). The electron energy increases and its trajectory keeps around the z axis. This can be explained by the fact that the electron rides on the laser field with the help of static electric field in the proper phase and gains substantial energy, traveling with the driving laser pulse.

Figures 3–5(d) show the dominating effects of LMRA where the static electric field and self-generated axial magnetic field coexist. Here, because the dimensionless self-generated axial magnetic field ($b_{z\ \max}=1.6$) is much larger than the static electric field ($k_E=0.01$), the effects of the static electric field can be ignored.

To give a clear picture of the difference in performance between the CP laser and the LP laser, we plot $\gamma \sim b_z$, i.e., the normalized energy (units of mc^2) with respect to the normalized magnetic field (unit=100 MG) with different laser intensity, for the case of the plane wave lasers and a constant axial magnetic field, in Fig. 6, where the analytic work is given by Salamin and Faisal [19]. Figures 6(a) and 6(b) are for the CP laser case. If we assume the constant magnetic field is parallel to the laser propagation direction, then $\gamma \sim b_z$ is shown in Fig. 6(a) for the right-hand CP, in Fig. 6(b) for the left-hand CP, and in Fig. 6(c) for the LP laser. An obvious resonance behavior can be observed near the resonance point, i.e., the dimensionless magnetic field

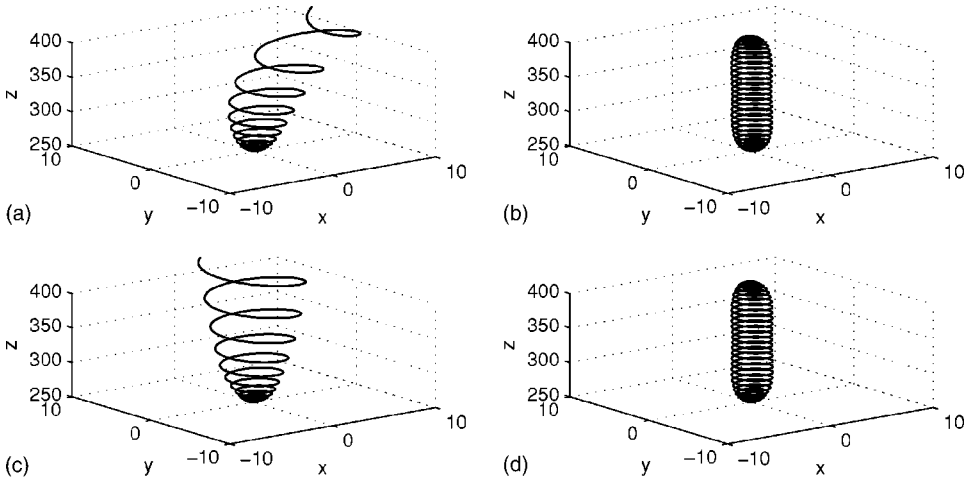

FIG. 5. The 3D electron trajectories (in the units of k^{-1}) with the same parameters of Figs. 2(a)–2(d), respectively.

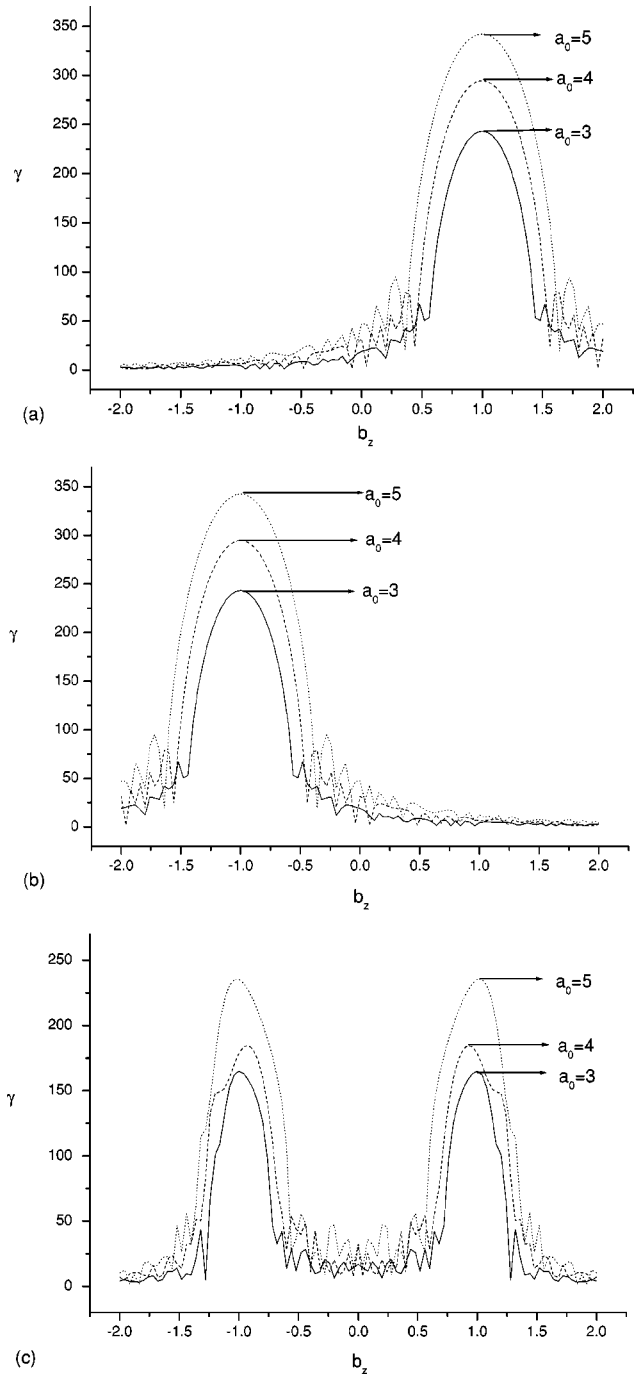

FIG. 6. $\gamma \sim b_z$ line of normalized energy along with normalized static magnetic field (unit=100 MG) with the different intensity a of plane wave laser. The dot line $a=5$, the dash line $a=4$, and the solid line $a=3$. The initial position starts from $\mathbf{r}=\mathbf{v}=0$ when $t=0$. Each achievable value γ is obtained at the same time $t=600$ in the units of ω^{-1}. (a) Right-hand CP laser. (b) Left-hand CP laser. (c) LP laser.

$b_z(=eB_z/m_ec\omega)$ equals the classical Larmor frequency Ω $(=eB_z/m_ec)$ of electron. The electron gains energy efficiently near the resonance point $(\Omega \approx b_z)$. The resonance regimes can be typically classified into three regimes: (a) exact resonance, (b) off-resonance $(b_z=0)$, (c) far away from resonance (only for CP laser). In the regime (c), at the magnetic field corresponding to the disappeared resonance peak of the LP laser case, we find that energetic electrons can be successively collimated and accelerated to a moderate energy <2 MeV. This kind of energetic electrons are suitable for the fast-ignitor ICF scheme.

III. DISCUSSIONS AND CONCLUSIONS

Using a single test electron model, we investigate the acceleration mechanism of energetic electrons in combined strong axial magnetic fields and circularly polarized laser fields. The axial magnetic field is considered as a constant field and a quasistatic axial magnetic field with Gaussian profile, respectively. An analytic solution of electron energy is obtained, showing a good agreement with numerical simulations for the physical parameters available for laboratory experiments. We find that the electron acceleration depends not only on the laser intensity, known as the pondermotive acceleration, but also on the ratio between electron classical Larmor frequency and the laser frequency. As the ratio approaches unity, a clear resonance peak is observed, that is, the LMRA. Away from the resonance regime, the strong magnetic fields still affect electron acceleration dramatically.

In contrast to the resonance acceleration described in Ref. [15] which dominates static electric field, our LMRA mechanism dominates in the case of strong quasistatic magnetic fields. In fast-ignitor scheme, there exists a high self-generated axial magnetic field if the CP laser is used. This fact provides an opportunity to acquire electrons with suitable energy.

To illustrate the difference between the CP laser and the LP laser, we plot the plane wave LP and CP laser of normalized electron energy with respect to the normalized static magnetic field, respectively. In the CP laser system there is only one resonance peak, whereas in the LP laser case there are two apparent resonance peaks. Obviously the electron energy gain increases with the intensity of the laser. In the CP laser system, the maximum energy will be higher than in LP case by about 20%. So the efficiency of energy transfer will be higher than in LP case.

In summary, the resonance acceleration mechanism of electrons in combined intense laser fields and strong magnetic fields (LMRA) is discussed in this paper. In absence of magnetic fields $(b_z=0)$, the electrons gain energy through usual ponderomotive acceleration that has been discussed extensively. In this case the laser polarization is not important, because the ponderomotive potential makes transverse momentum of energetic electrons equal in x-axis and y-axis direction. For this reason, the LP laser has been discussed thoroughly in recent years whereas the CP laser is relatively seldom mentioned. However, the fast ignition scheme requires the electrons with energy less than 2 MeV to match the stopping distance in compressed DT fuel core, which seems not easily satisfied by the LP laser system. In the present paper we turn to investigate the CP laser combined with strong quasistatic magnetic fields. We find that in the CP laser system there is only one resonance peak, while in the LP laser system there are two resonance peaks. More

importantly, at the magnetic field corresponding to the disappeared resonance peak, the energetic electrons can be successively collimated and accelerated to a moderate energy (<2 MeV), with an intense CP laser ($I>10^{18}$ W/cm^2) and axial self-generated quasistatic magnetic field ($Bs\approx 10^8$ G). This kind of energetic electrons have potential applications in the fast-ignitor scheme of ICF.

ACKNOWLEDGMENTS

H.L. thanks J. Liu for revising the manuscript. This work was supported by National Hi-Tech Inertial Confinement Fusion Committee of China, National Natural Science Foundation of China, National Basic Research Project "nonlinear Science" in China, and National Key Basic Research Special Foundation.

[1] A. Pukhov, Rep. Prog. Phys. **66**, 47 (2003).
[2] Dong Lai, Rev. Mod. Phys. **73**, 629 (2001).
[3] A. Pukhov and J. Meyer-ter-Vehn, Phys. Plasmas **5**, 1880 (1998).
[4] Mitsumori Tanimoto *et al.*, Phys. Rev. E **68**, 026401 (2003).
[5] Shi-Bing Liu, Shi-Gang Chen, and Jie Liu, Phys. Rev. E **55**, 3373 (1997).
[6] L. Gorbunov, P. Mora, and T. M. Antonsen, Phys. Rev. Lett. **76**, 2495 (1996).
[7] Z. M. Sheng and J. Meyer-ter-Vehn, Phys. Rev. E **54**, 1833 (1996).
[8] R. N. Sudan, Phys. Rev. Lett. **70**, 3075 (1993).
[9] Shao-ping Zhu, X. T. He, and C. Y. Zheng, Phys. Plasmas **8**, 321 (2001).
[10] M. Tatarakis *et al.*, Nature (London) **415**, 280 (2002).
[11] M. Tabak *et al.*, Phys. Plasmas **1**, 1626 (1994).
[12] M. Tatarakis *et al.*, Phys. Rev. Lett. **81**, 999 (1998).
[13] G. Malka *et al.*, Phys. Rev. E **66**, 066402 (2002).
[14] A. Pukhov and J. Meyer-ter-Vehn, Phys. Rev. Lett. **76**, 3975 (1996).
[15] M. Schmitz and H.-J. Kull, Laser Phys. **12**, 443 (2002).
[16] Y. Horovitz *et al.*, Phys. Rev. Lett. **78**, 1707 (1997).
[17] Z. Najmudin *et al.*, Phys. Rev. Lett. **87**, 215004 (2001).
[18] F. V. Hartemann *et al.*, Phys. Rev. E **51**, 4833 (1995).
[19] Yousef I. Salamin and Farhad H. M. Faisal, Phys. Rev. A **58**, 3221 (1998).